IET Communications

Research Article

Iterative smoothing filtering schemes by using clipping noise-assisted signals for PAPR reduction in OFDM-based carrier aggregation systems

ISSN 1751-8628
Received on 22nd May 2018
Revised 20th November 2018
Accepted on 30th January 2019
E-First on 26th February 2019
doi: 10.1049/iet-com.2018.5421
www.ietdl.org

Shu-Ping Lin[1], Yung-Fang Chen[1] ✉, Shu-Ming Tseng[2]
[1]*Department of Communication Engineering, National Central University, Taiwan*
[2]*Department of Electronic Engineering, National Taipei University of Technology, Taiwan*
✉ *E-mail: yfchen@ce.ncu.edu.tw*

Abstract: Aggregating a lot of subcarriers will generate high peak-to-average power ratio (PAPR) which makes the overall system performance degradation. Among the existing PAPR reduction methods for orthogonal frequency-division multiplexing (OFDM)-based systems, iterative clipping and filtering (ICF) may be easy to implement, but ICF may cause signal distortion, so that the system cannot approximate the processed signals to the original signals which degrades error rates at receivers. Here, the authors proposed a new method based on ICF with smoothed clipping signals, and find the optimised filter to achieve the minimum error vector magnitude and efficiently reduce PAPR. Owing to the lack of a wide range of continuous bandwidth, the Third Generation Partnership Project proposed carrier aggregation (CA) technology in LTE-advanced systems. CA can aggregate many contiguous or non-contiguous fragment spectrums for supporting larger bandwidth and higher peak data rate. Here, the authors also evaluate the developed PAPR reduction scheme for the use in CA scenarios. The efficacy of the proposed scheme is demonstrated in the simulation results.

1 Introduction

In order to meet the demand of high date rate requirements, the Third Generation Partnership Project (3GPP) has proposed long-term evolution-advanced (LTE-A) which supports peak data rates of 1 Gbps in the downlink and 500 Mbps in the uplink [1]. However, rare network operators can get a large continuous bandwidth to fulfil the LTE-A system standard. Carrier aggregation (CA) is a key technology of LTE-A through aggregating two or more contiguous or non-contiguous component carriers (CCs) in different operating bands for supporting large bandwidth and high peak data rate while preserving backward compatibility to Release 8 and 9 LTE systems [2].

A practical problem of CA is the significant increase in the peak-to-average power ratio (PAPR) in the time-domain signals [3, 4]. Higher PAPR may be created when more CCs are aggregated. For mobile users, PAPR is one of the major problems to affect system performance in the CA technology. High PAPR results in significant non-linear distortion where the signal is operated at a non-linear region of power amplifier (PA). It degrades the bit-error-rate (BER) performance. If we reduce the PAPR of the multicarrier signals in the baseband, the impact of the abovementioned would be mitigated. Many approaches have been proposed to reduce the PAPR of orthogonal frequency-division multiplexing (OFDM)-based signals at the expense of transmit signal power increase, data rate loss, computational complexity increase, BER increase, or code rate loss [5, 6].

These varied methods basically can be divided into three major categories: clipping, coding, and scrambling techniques. The clipping techniques, including amplitude clipping and clipping along with filtering, clip the OFDM signals to a predefined threshold to reduce PAPR effect [7–10]. These techniques are easy to implement, but they may cause in-band distortion and out-of-band radiation, which would increase BER and adjacent channel interferences. The coding technique uses exhaustive search to find the codeword with the minimum PAPR for transmission. This technique suffers from bandwidth efficiency loss as the code rate is reduced and it may need to store large lookup tables for encoding and decoding processes [11–13]. The scrambling techniques, including tone reservation (TR) [14, 15], tone injection (TI) [16], interleaving, selected mapping (SLM) [17–19], and partial transmit sequence (PTS) [20–22], scramble the OFDM symbols by adding signals or multiplying a set of phases to find the minimum PAPR and transmit the associated signal. The scrambling and the coding techniques are appropriate to a small number of subcarriers because their complexities increase accordingly when the number of subcarriers increases. Therefore, to avoid bandwidth efficiency loss and too much extra storage usage, in this paper, we focus on the clipping-based techniques to reduce PAPR. Recently, some other types of PAPR reduction algorithms are proposed. In [23], the authors proposed a PAPR reduction method by randomly signal constellation mapping. Then the candidate symbol with the lowest PAPR is sent out along with its candidacy number. Thus, the scheme requires additional bandwidth. In [24], it proposed a hybrid scheme to reduce PAPR for filter bank multicarrier (FBMC) system by using the combination of a discrete sine transform precoding technique and an A-Law non-linear companding technique. In [25], alternatively, a novel processing scheme performed at the receiver is proposed where the proposed clipping noise cancellation scheme is to recreate the clipping process at the receiver using detected symbols, then estimate and cancel the frequency-domain clipping noise caused by it.

In this paper, as abovementioned, we consider utilising both clipping signals and clipping noises along with a filter design. We propose a new scheme based on iterative clipping and filtering (ICF) [26] where we replace the classic clipping and the rectangular window filter by a clipping noise vector-assisted signal along with an optimal filter to make the constellation points of the clipped signal back to ideal location approximately. The proposed scheme has better performance in terms of reduced PAPR and BER while being compared with the existing ICF techniques. The major contribution of this work is to propose a novel PAPR reduction scheme based on clipping and filtering techniques for OFDM-based systems. The proposed iterative smoothed clipping and optimised filtering (ISCOF)-based scheme does not require code books, overhead, and additional bandwidths which is different from other types of PAPR reduction schemes. The proposed scheme provides better performance in terms of PAPR and BERs and has a comparable complexity compared with the counterparts. The

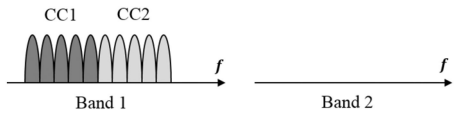

Fig. 1 *Intra-band contiguous CA*

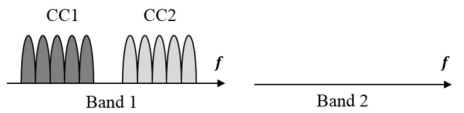

Fig. 2 *Intra-band non-contiguous CA*

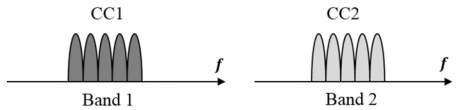

Fig. 3 *Inter-band non-contiguous CA*

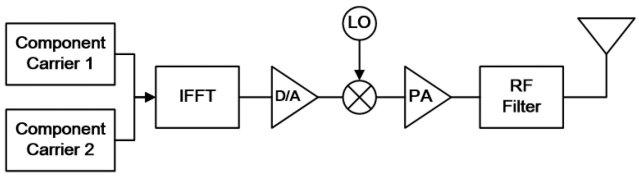

Fig. 4 *Transmitter architecture option A*

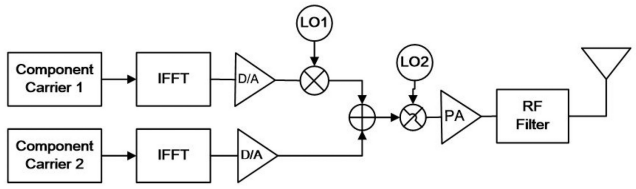

Fig. 5 *Transmitter architecture option B*

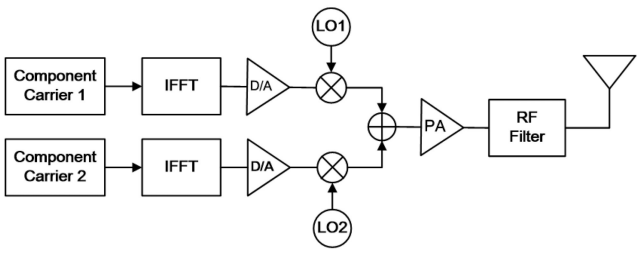

Fig. 6 *Transmitter architecture option C*

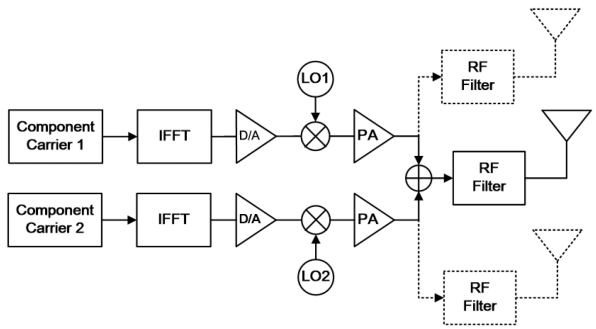

Fig. 7 *Transmitter architecture option D*

application of the proposed scheme is evaluated for the scenarios of CA. The proposed scheme can also be applied in non-CA systems and the scenarios of CA are applied and presented.

The rest of this paper is organised as follows. In Section 2, we introduce the scenarios of CA and the architectures of transmitter and receiver, and describe PAPR in systems. The proposed PAPR reduction scheme is presented in Section 3 and the complexity analysis of the proposed scheme appears in Section 4. In Section 5, simulation results are presented. Finally, we make a conclusion in Section 6

2 CA and PAPR in multicarrier systems

LTE-A, which has been proposed by 3GPP in Release 10, aims to support peak data rates of 1 Gbps on downlink and 500 Mbps on uplink. To meet the above requirements, the transmission bandwidth should be up to 100 MHz. However, it may not be available to have such large contiguous spectrum in reality. LTE-A introduces CA to extend the overall bandwidth in order to provide the targeted data rate [27, 28]. The aggregated carrier is CC which is backward compatible with Release 8 and 9 LTE. The CC can have the bandwidth of 1.4, 3, 5, 10, 15, or 20 MHz and a maximum of five CCs can be aggregated. The operators can aggregate two or more CCs in the same or different bands to serve a mobile user. If the traffic demand is high, the operators can dynamically allocate a larger bandwidth to fulfil the user's requirements. There are three different spectrum scenarios as shown in Figs. 1–3:

i. *Intra-band contiguous CA:* The CCs are adjacent to each other in the same operating band as shown in Fig. 1. The aggregated channel can be regarded as a single enlarged channel from the RF view point, so only one transceiver is required in the terminal or UE. The spacing between centre frequencies of contiguous CCs should be a multiple of 300 kHz which is compatible with the 100 kHz frequency raster of LTE Rel-9 and preserves orthogonality of the subcarriers with 15 kHz spacing [29].
ii. *Intra-band non-contiguous CA:* The CCs belong to the same operating band, but have a gap or gaps in each CC as shown in Fig. 2. As the contiguous spectrum resource is rarely available, the non-continuous CA provides a practical approach to fully utilise fragment spectrum. This scenario is more complicated than the contiguous one. The multicarrier signal cannot be treated as a single signal, so multiple transceivers are required. This would increase cost to the UE.
iii. *Inter-band non-contiguous CA:* The CCs use different operating bands as Fig. 3. Mobile receivers can take advantage of different radio propagation characteristics in different bands. For the UE, it needs to use multiple transceivers within the UE device.

The 3GPP proposes various transmitter architectures in [30, 31] where the CCs are combined to support the different type of CAs, i.e. at digital baseband (option A), or in analogue waveforms before RF mixer (option B), or after mixer but before the PA (option C), or after the PA (option D) as shown in Figs. 4–7. The authors in [32, 33] illustrate two receiver architectures where the carriers are separated from each other, i.e. at a digital baseband (option A) or at an RF chain (option B).

Multicarrier technologies in the form of OFDMs are being standardised for wireless communication systems in 4G and 5G. Although OFDM offers many advantages, there is a problem of high PAPR which makes signals suffer from non-linear effects of PAs.

For a discrete time signal $x(n)$, the PAPR is defined as the ratio of the maximum power to the average power

$$\begin{aligned}\mathrm{PAPR} &= \frac{\max_{n=1\ldots N}|x(n)|^2}{E\left[|x(n)|^2\right]} = \frac{\max_{n=1\ldots N}|x(n)|^2}{(1/N)\sum_{n=1}^{N}|x(n)|^2} \\ &= \frac{\|x(n)\|_\infty^2}{(1/N)\|x(n)\|_2^2}\end{aligned} \tag{1}$$

where $E\left[|x(n)|^2\right]$ is the average power of the signal, $\|\cdot\|_2$ the 2-norm, and $\|\cdot\|_\infty$ the ∞-norm.

The PAPR is often described in statistics. The complementary cumulative distribution function (CCDF) is one of the commonly used performance measures for PAPR reduction techniques. The CCDF of PAPR denotes the probability that the PAPR of the signal

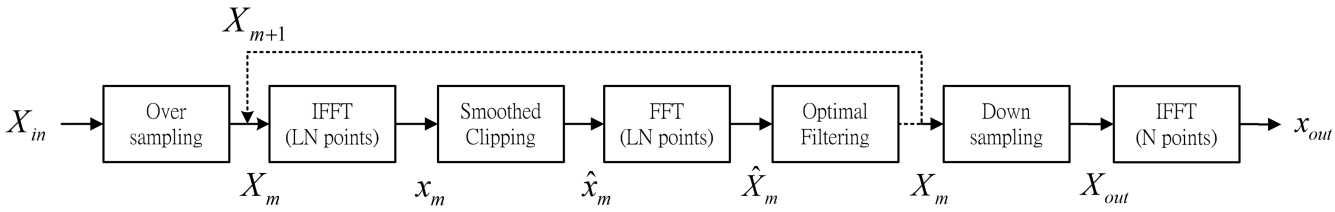

Fig. 8 *Iterative smoothed clipping and optimal filtering scheme*

exceeds a given threshold. The CCDF of $x(n)$ with an event regarding a specific threshold (Th) was given as

$$\text{CCDF} = \text{Prob}(\text{PAPR} > \text{Th}) = 1 - \left(1 - \mathrm{e}^{-\text{Th}}\right)^N. \tag{2}$$

For a particular standard, a circular shift-based reduced PAPR method has been applied to solve the PAPR problem [34].

3 Proposed PAPR reduction scheme

Clipping and filtering might be the simplest technique for PAPR reduction. However, clipping may cause in-band distortion and out-of-band radiation. Particularly, the in-band distortion degrades BER performance of the OFDM signals. One solution is to reconstruct the signal by the clipped samples based on the other samples in the oversampled signals. On the other hand, the out-of-band radiation reduces spectral efficiency. The frequency-domain filtering after the clipping can eliminate the out-of-band radiation, but this filtering may lead to some time-domain peaks regrowth. To reduce those higher peaks that occurs after the filtering, an iterative method of clipping and filtering (ICF) can be used to suppress the peak regrowth [26, 35, 36].

In recent years, convex optimisation has been widely used in communication signal processing. Wang and Luo [37] propose a convex optimisation algorithm called optimised ICF (OICF) to develop a frequency-domain optimal filter which is applied to the clipped signals in order to minimise the number of iterations. Another simplified optimised ICF (SICF) scheme is proposed in [38] which concentrates the attention on manipulating the clipping noise with a lower computational complexity and the slightly worse performance than OICF.

In this paper, we develop an ISCOF-based PAPR reduction algorithm by processing both the clipped signal and the clipping noise which is different from the approaches in [37, 38]. The block diagram of the proposed scheme is shown in Fig. 8, where

$$\boldsymbol{X}_{\text{in}} \in C^N, \boldsymbol{X}_m \in C^{LN}, \boldsymbol{x}_m \in C^{LN}, \hat{\boldsymbol{x}}_m \in C^{LN},$$
$$\hat{\boldsymbol{X}}_m \in C^{LN}, \boldsymbol{X}_{\text{out}} \in C^N, \boldsymbol{x}_{\text{out}} \in C^N$$

and $m = 1, 2, \ldots, M$ denotes the number of iterations and M is the maximum number of iterations. Referring to Fig. 8, the difference of the process from [37] is that the proposed method utilises the clipped noise in the optimal filtering processing.

In the following discussion, the symbols with boldface denote the associated vector forms. In OFDM systems, orthogonal subcarriers are used to transmit data symbols. The N data symbols $X(n)$, $n = 0, 1, \ldots, (N-1)$, which are carried by N subcarriers, form a data block $\boldsymbol{X} = [X(0), X(1), \ldots, X(N-1)]$. Then, the time-domain OFDM symbol $x(k)$ with L times oversampling is expressed as

$$x(k) = \frac{1}{\sqrt{LN}} \sum_{n=0}^{N-1} X(n)\, \mathrm{e}^{\mathrm{j}(2\pi/LN)nk}, \quad k = 0, 1, \ldots, LN-1 \tag{3}$$

The frequency-domain downsampling OFDM symbol $X(n)$ can be obtained by

$$X(n) = \frac{1}{\sqrt{LN}} \sum_{n=0}^{LN-1} x(k)\, \mathrm{e}^{-\mathrm{j}(2\pi/LN)nk}, \quad n = 0, 1, \ldots, N-1 \tag{4}$$

The oversampling operation is achieved by zero-padding. For example, we add $N(L-1)$ zeros to the end of $X(n)$ to get $\boldsymbol{X} = [X(0), X(1), \ldots, X(N-1), 0, 0, \ldots, 0]$ [38].

First, we consider manipulating clipping noises to propose a method for reconstructing the smoothed clipping signals. We defined $\boldsymbol{c}_m$ as the difference between the predefined threshold (Th) and the incoming signal at the mth iteration

$$c_m(k) = \begin{cases} 0 & |x_m(k)| \le \text{Th} \\ (|x_m(k)| - \text{Th})\mathrm{e}^{\mathrm{j}\theta_m(k)}, & |x_m(k)| > \text{Th} \end{cases} \tag{5}$$

where $k = 0, 1, \ldots, LN-1$ and $\theta_m(k)$ is the phase of $x_m(k)$.

The clipping threshold is calculated by a parameter called clipping ratio (CR) which is related to the desired PAPR (denoted $\text{PAPR}_{\max}$)

$$\text{CR} = \sqrt{\text{PAPR}_{\max}} \tag{6}$$

$$\text{Th} = \frac{1}{\sqrt{LN}} \| x_m(k) \|_2 CR \tag{7}$$

Equation (5) is rewritten into (8) when we focus on the peaks which exceed the threshold

$$c_m(k_p) = \left(|x_m(k_p)| - \text{Th}\right) \mathrm{e}^{\mathrm{j}\theta_m(k_p)} \tag{8}$$

and we assume there are P peaks exceeding the threshold at indexes $k = k_1, k_2, \ldots, k_P$.

As similar to [18], a normalised frequency-domain basic vector $\boldsymbol{B}_n$ with N ones and $N(L-1)$ zeros is

$$\boldsymbol{B}_n = \frac{1}{\| \boldsymbol{b}_n \|_\infty} [1, \ldots, 1, 0, \ldots, 0] \tag{9}$$

where $\boldsymbol{b}_n$ is the time-domain signal of the frequency-domain basic vector $[1, \ldots, 1, 0, \ldots, 0]$ and $\| \boldsymbol{b}_n \|_\infty$ denotes the largest value of $\boldsymbol{b}_n$.

Then, by converting $\boldsymbol{c}_m$, the vector form of (8), to the frequency-domain yielding $\boldsymbol{C}_m$ and multiplying $\boldsymbol{C}_m$ by the basic vector $\boldsymbol{B}_n$, we have the frequency-domain clipping noise vector $\hat{\boldsymbol{C}}_m$

$$\hat{\boldsymbol{C}}_m = \boldsymbol{C}_m \boldsymbol{B}_n \tag{10}$$

Hence, the clipping operation is performed as

$$\hat{\boldsymbol{x}}_m = \boldsymbol{x}_m - \text{IFFT}(\hat{\boldsymbol{C}}_m) = \boldsymbol{x}_m - \hat{\boldsymbol{c}}_m \tag{11}$$

Fig. 9 is an illustration of a clipping noise vector $\hat{\boldsymbol{c}}_m$. Referring to Fig. 9, the amplitude of each peak is the difference between the threshold and the signal peak. As the signals at the around peaks are decaying and fluctuating slowly, the clipped signal $\hat{x}_m$ will be a smoother version compared with the original signal than a flat clipped signal as shown in Fig. 10.

In order to let the constellation points of clipped signals back to the original location approximately, an optimal filter is thus developed to compensate the distortion of the clipped signals in the proposed processing procedures by utilising the similar approach in [37]. The error vector magnitude (EVM) is used to quantify the amount of in-band distortion for the processed OFDM symbol. A signal sent by an ideal transmitter is mapped precisely to the

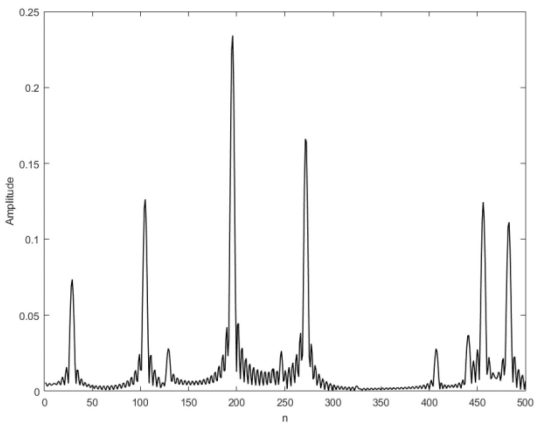

Fig. 9 *Example of a clipping noise vector* $\hat{\boldsymbol{c}}_m$

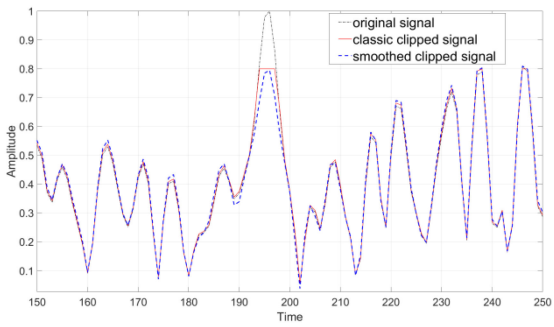

Fig. 10 *Comparison of a classic and a smoothed clipping signals*

Table 1 Computational complexity comparison

Scheme	Computational complexity
ICF [26]	$O(2MLN\log_2(LN)+4MLN)$
OICF [37]	$O(MN^3+(M+1)LN\log_2(LN)+2MLN)$
SICF [38]	$O((M+1)LN\log_2(LN)+4MLN)$
proposed	$O(MN^3+(2M+1)LN\log_2(LN)+4MLN)$

associated constellation points. However, various imperfect processes cause the actual constellation points to deviate from the ideal locations. The difference between the ideal constellation points and the deviated points is called the error vector. For a single OFDM symbol, the EVM is defined as the squared root of the ratio of the mean error vector power to the mean reference power

$$\mathrm{EVM}=\sqrt{\frac{(1/N)\sum_{n=0}^{N-1}|X_{\mathrm{in}}(n)-X_{\mathrm{out}}(n)|^2}{(1/N)\sum_{n=0}^{N-1}|X_{\mathrm{in}}(n)|^2}}=\frac{\|\boldsymbol{X}_{\mathrm{in}}-\boldsymbol{X}_{\mathrm{out}}\|_2}{\|\boldsymbol{X}_{\mathrm{in}}\|_2} \quad (12)$$

where $X_{\mathrm{in}}(n)$ and $X_{\mathrm{out}}(n)$ denote the ideal and the deviated data symbols. $\boldsymbol{X}_{\mathrm{in}}$ and $\boldsymbol{X}_{\mathrm{out}}$ are their associated vector form.

The optimal filter is proposed to dynamically modify the filter response at each iteration and is solved by the formulation as follows:

$$\begin{aligned}
\min_{\boldsymbol{H}\in C^N} \quad & \mathrm{EVM}=\frac{\|\boldsymbol{X}_{\mathrm{in}}-\boldsymbol{X}'_m\|_2}{\|\boldsymbol{X}_{\mathrm{in}}\|_2}\\
\text{subject to} \quad & \boldsymbol{X}'_m=\hat{\boldsymbol{X}}'_m\cdot\boldsymbol{H}\\
& \boldsymbol{X}''_m=0 \qquad (13\text{a–e})\\
& \boldsymbol{x}_{m+1}=\mathrm{IFFT}(\boldsymbol{X}_m)\\
& \frac{\|\boldsymbol{x}_{m+1}\|_\infty}{(1/\sqrt{LN})\|\boldsymbol{x}_{m+1}\|_2}\le\sqrt{\mathrm{PAPR}_{\max}}=CR
\end{aligned}$$

where $\hat{\boldsymbol{X}}_m=[\hat{\boldsymbol{X}}'_m;\hat{\boldsymbol{X}}''_m]$ and $\boldsymbol{X}_m=[\boldsymbol{X}'_m;\boldsymbol{X}''_m]$ denote the frequency-domain symbols before and after the filtering procedure. $\boldsymbol{H}$ is formed by the coefficients of the filter. $\hat{\boldsymbol{X}}'_m$ and $\boldsymbol{X}'_m$ are the in-band $(0\le k\le N-1)$ components. $\hat{\boldsymbol{X}}''_m$ and $\boldsymbol{X}''_m$ are the out-of-band $(N\le k\le LN-1)$ components. The operator '·' denotes element-by-element product.

The optimisation model (13) is non-convex because the constraint function (13) is non-convex. To modify the optimisation problem into a convex formulation, we approximate $\|\boldsymbol{x}_{m+1}\|_2$ by $\|\hat{\boldsymbol{x}}_m\|_2$. The non-convex constraint can be turned into a convex constraint by (7)

$$\|\boldsymbol{x}_{m+1}\|_\infty\le\mathrm{Th}_{m+1}=\sqrt{\frac{1}{LN}}\|\hat{\boldsymbol{x}}_m\|_2CR \quad (14)$$

Then, a matrix $\boldsymbol{A}$ is defined which consists of the first N columns of LN–IFFT matrix, and a variable t to replace EVM. With these adjustments, the optimisation problem (13) is translated into a second-order cone programming (SOCP) [39]

$$\begin{aligned}
\min_{\boldsymbol{H}\in C^N,\,t\in R} \quad & t\\
\text{subject to} \quad & \|\boldsymbol{X}_{\mathrm{in}}-\hat{\boldsymbol{X}}'_m\cdot\boldsymbol{H}\|_2\le\|\boldsymbol{X}_{\mathrm{in}}\|_2 t \qquad (15\text{a–c})\\
& \left|\boldsymbol{A}(\hat{\boldsymbol{X}}'_m\cdot\boldsymbol{H})\right|\le\sqrt{\frac{1}{LN}}\|\hat{\boldsymbol{x}}_m\|_2CR
\end{aligned}$$

The convex optimisation problem can be solved by using the public software CVX [40].

4 Complexity analysis

The Big-Oh notation is used to analyse the complexity of the algorithms. In the proposed scheme, the complexity of computing (5) and (7) is $O(LN)$. FFT operation is performed to yield $\boldsymbol{C}_m$. However, the value of P is much less than LN, so the inputs of the FFT used to compute $\boldsymbol{C}_m$ are sparse. Therefore, the complexity of (10) can be reduced to $O(LN)$ by using the wavelet transform [41]. In (11), the complexity is $O(LN\log_2(LN)+LN)$. The cost of solving the optimisation SOCP model is $O(N^3)$. Based on the above analysis, the overall computational complexity of the first iteration is $O(N^3+3LN\log_2(LN)+4LN)$. In the subsequent iterations, the computational complexity can be reduced to $O(N^3+2LN\log_2(LN)+4LN)$. Finally, the computational complexity of the proposed scheme with M iterations is $O(MN^3+(2M+1)LN\log_2(LN)+4MLN)$. The computational complexities of ICF, OICF, SICF, and the proposed schemes in terms of the Big-Oh notation are compared in Table 1. The scheme [37] offered the best performance among the existing algorithms except the proposed algorithm. Our proposed algorithm has a comparable computational complexity and offers better performance than that of [37].

5 Simulation results

In order to compare the performance of the existing and the proposed schemes, this section shows the simulation results in different scenarios. The simulations are conducted by using the Matlab software tool in a PC-based window environment. The matlab code may be rewritten and translated into other platforms for real-time applications. The desired PAPR is set to 5 dB; each CC has a bandwidth of 5 MHz, 300 subcarriers, QPSK modulation, and the oversampling factor L is 4.

5.1 Contiguous CA

For the intra-band contiguous scenario, the transmitter architecture of Fig. 4 is well suited to apply. There are two ways, labelled type I and type II, regarding aggregating CCs before the PAPR reduction procedure.

The first aggregating operation is implemented as shown in Fig. 11 for type I. We use two contiguous CCs in our simulation.

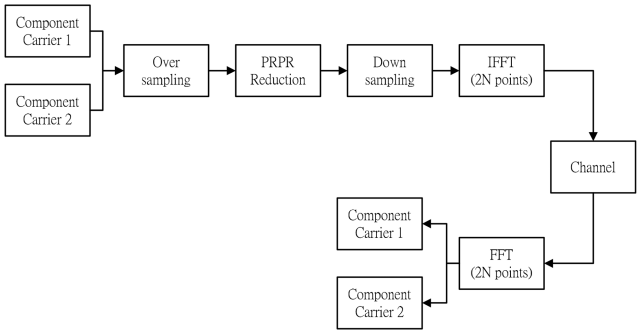

Fig. 11 *Block diagram of type I for continuous CA*

Table 2 Performance of type I at one and two iterations

Scheme	*m*	PAPR, dB	EVM, %
ICF	1	6.6556	7.16
	2	6.0747	9.20
OICF	1	5.0455	8.20
	2	4.9613	8.55
SICF	1	5.8033	7.52
	2	5.4626	8.17
proposed scheme	1	4.8334	8.35
	2	4.4780	8.68

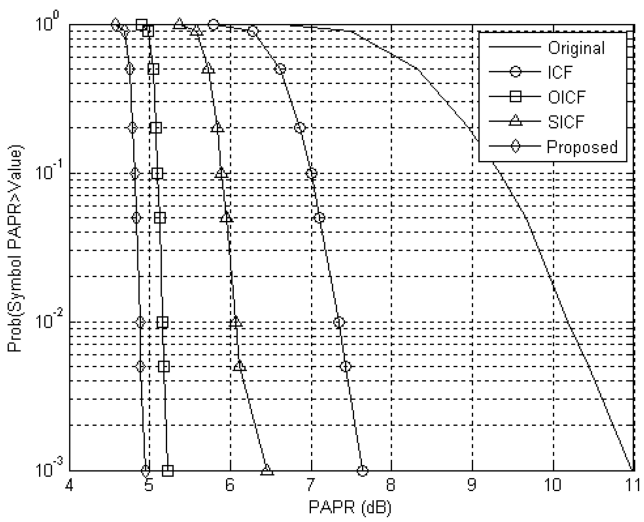

Fig. 12 *PAPR comparison of four schemes with two contiguous CCs (type I)*

CC1 and CC2 are put side by side in the frequency-domain to form an aggregated signal with twice bandwidth.

Table 2 shows the performance comparison of all schemes with one and two iterations. The desired PAPR is set to 5 dB. The PAPR of the original signal is 8.5412 dB. The proposed scheme (ISCOF) has a low PAPR which is smaller than the desired PAPR at the first iteration; the others should iterate more than three times in order to achieve the desired PAPR. The PAPR is inversely proportional to the EVM roughly. The EVM becomes larger while increasing the number of iterations as the clipping process would cause more distortion. The optimal filter can mitigate the increment of the EVM at the next iteration.

The CCDF of the PAPR reduction schemes with 1000 trials is displayed for performance comparison as shown in Fig. 12. All schemes can significantly reduce the PAPR of the OFDM signals. The proposed scheme provides ~6.037 dB PAPR reduction and OICF achieves ~5.76 dB PAPR reduction at a CCDF probability of 10^{-3} at one iteration. The additional 0.277 dB gain by using the proposed scheme is due to the smoothed clipping which reduces the in-band distortion and out-of-band radiation.

Fig. 13 shows the BER curves of the original signals and the modified signals with the existing and the proposed schemes in an

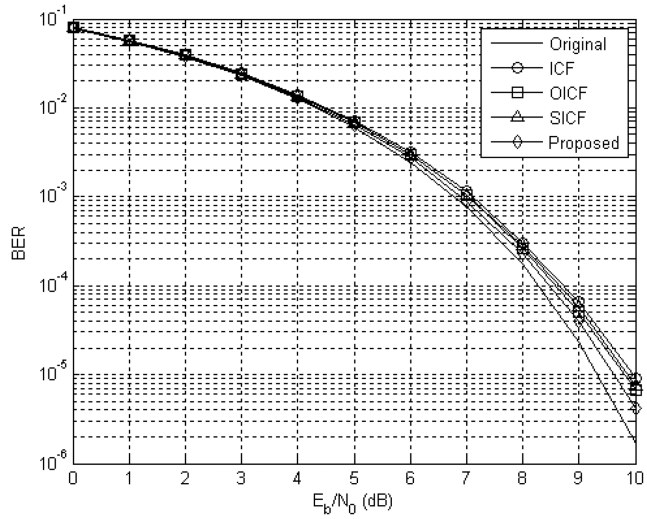

Fig. 13 *BER performance of four schemes with two contiguous CCs (type I)*

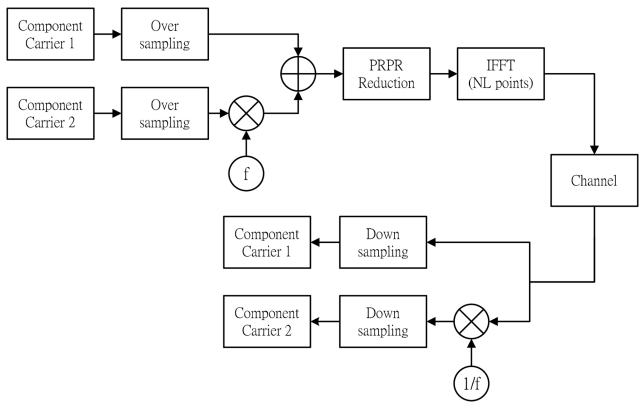

Fig. 14 *Block diagram of type II for continuous CA*

additive white Gaussian noise channel at one iteration. All BER curves of the modified signals are located at the right side of the original signal's curve because the related clipping procedures causes signal distortion. The BER performance of the proposed scheme is better than those of the other existing schemes. By taking an example, at a BER level of 10^{-5}, OICF yields ~0.0858 dB worse than the proposed scheme, and SICF results in 0.1135 dB worse than the proposed scheme. It demonstrates that the proposed smoothed clipping method has less distortion than the other schemes.

The other aggregating operation is implemented as shown in Fig. 14 for type II. We multiply CC2 with a complex number $e^{j2\pi ft}$ to change the centre frequency of CC2. Adding CC1 and CC2 forms an aggregated signal. The aggregated signal is transmitted by the oversampling with *LN* points and the downsampling operation is performed at the receiver end.

Table 3 compares the performance of all schemes with one and two iterations and the desired PAPR is set to 5 dB. The PAPR of the original signal is 8.6903 dB. The performance trend is quite similar to that of type I.

Figs. 15 and 16 show the performance of type II at one iteration. The performance trend is similar to that of type I. The proposed scheme has better performance.

5.2 Non-contiguous CA

In the non-contiguous scenario, each CC in the baseband is processed individually and aggregated before or after the PA as shown in Figs. 5–7. It is processed in the same as the method of type I, but it may not be feasible with type II. For example, if CC1 is located in 1 GHz and CC2 in 2 GHz, the bandwidth of 1 GHz would be required for using type II to aggregate them. As each CC

Table 3 Performance of type II at one and two iterations

Scheme	*m*	PAPR, dB	EVM, %
ICF	1	6.5498	4.69
	2	5.9020	6.71
OICF	1	5.7363	4.93
	2	5.6560	5.18
SICF	1	6.4621	4.68
	2	5.5282	6.30
ISCOF	1	5.5358	5.56
	2	5.4559	5.84

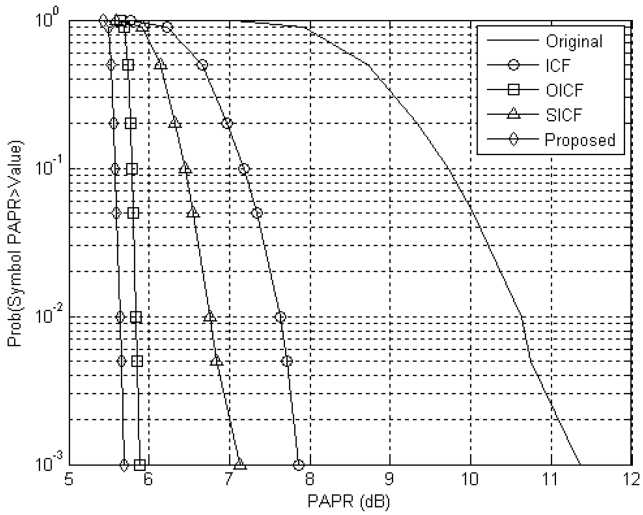

Fig. 15 *PAPR comparison of four schemes with two contiguous CCs (type II)*

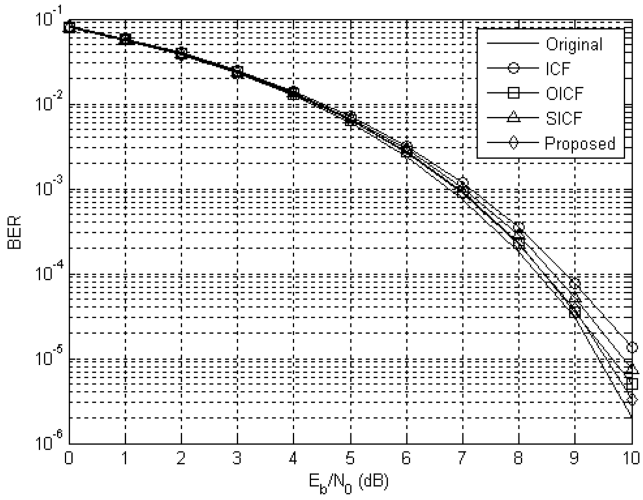

Fig. 16 *BER performance of four schemes with two contiguous CCs (type II)*

Table 4 Performance of NC CA at one and two iterations

Scheme	*m*	PAPR, dB	EVM, %
ICF	1	6.4742	15.41
	2	5.9496	17.61
OICF	1	5.0785	7.89
	2	4.9612	8.02
SICF	1	5.6614	10.81
	2	5.3693	11.63
ISCOF	1	4.8731	7.07
	2	4.8436	7.53

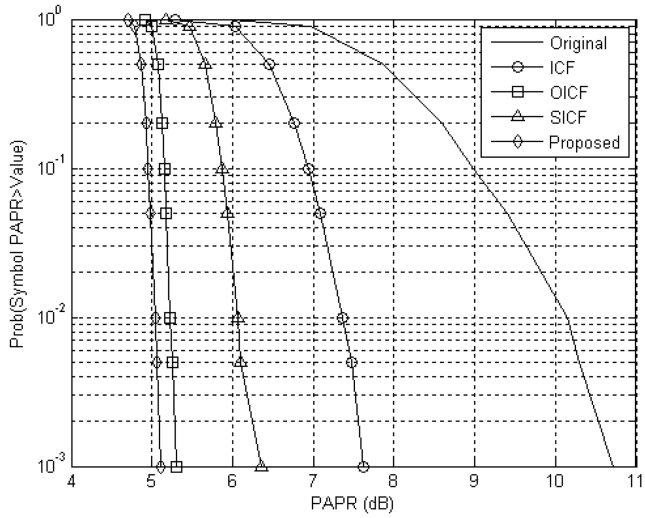

Fig. 17 *PAPR comparison of four schemes with non-contiguous CCs (type I)*

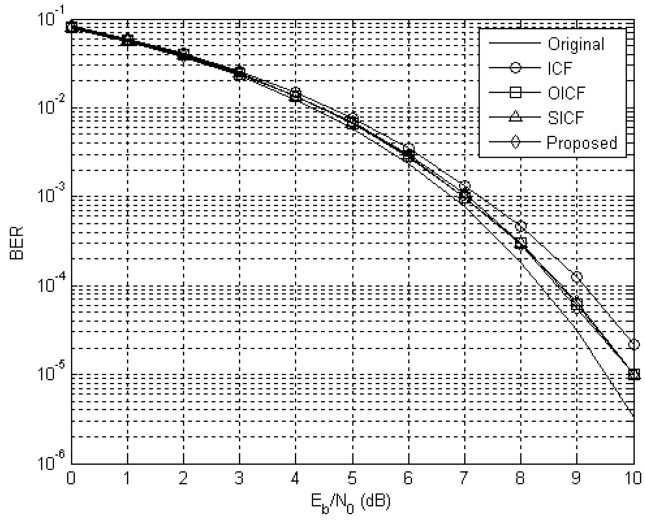

Fig. 18 *BER performance of four schemes with non-contiguous CCs (type I)*

is processed individually, the number of CCs does not have impact on the performance.

Table 4 compares the performance of all schemes with one and two iterations and the desired PAPR is set to 5 dB. The PAPR of the original signal is 7.9344 dB. Figs. 17 and 18 show the performance of PAPR and BER at one iteration. The proposed scheme still has better performance than the others.

6 Conclusion

The CA technology can aggregate many contiguous or non-contiguous bands to form a wide bandwidth, but the PAPR problem would become more serious. In this paper, we propose an ISCOF to efficiently reduce the PAPR with less distortion, minimum EVM, and offer better BER performance. The procedure of the smoothed clipping reduces the in-band distortion along with out-of-band radiation and it offers better BER performance. The optimal filter dynamically adjusts the filter response at each iteration under the constraints of the minimum EVM and the desired PAPR.

The simulation results compare the proposed scheme with the classic, the optimised, and the simplified ICF schemes. The proposed scheme has better performance in terms of PAPR reduction, BER, and EVM. With the help of the proposed scheme, the number of iterations required to achieve a given PAPR is significantly reduced. It almost requires only one iteration to reach the desired value in most cases. The scheme [37] offered the best performance among the existing algorithms except the proposed

algorithm. Our proposed algorithm has a comparable computational complexity and offers better performance than that of [37].

7 Acknowledgment

The authors would like to thank the Ministry of Science and Technology of the Republic of China, Taiwan, for financially supporting this research under Contract no. MOST 105-2221-E-008-013.

8 References

[1] 3GPP Technical Report 36.913: 'Requirements for further advancements for Evolved Universal Terrestrial Radio Access (E-UTRA) (LTE-Advanced)', v9.0.0, February 2010

[2] Al-Shibly, M.A.M., Habaebi, M.H., Chebil, J.: 'Carrier aggregation in long term evolution-advanced'. Proc. IEEE Control and System Graduate Research Colloquium (ICSGRC), Shah Alam, Selangor, Malaysia, July 2012, pp. 154–159

[3] Zeng, Q.Z., Shi, Z.P., Wang, W.T., *et al.*: 'Analyses of interferences between component carriers in carrier aggregation'. Proc. Third Int. Conf. on Communications and Mobile Computing (CMC), Qingdao, China, April 2011, pp. 420–423

[4] Yen, P., Minn, H., Chong, C.C.: 'PAPR reduction for bandwidth-aggregated OFDM and SC-FDMA systems'. Proc. IEEE Wireless Communications and Networking Conf. (WCNC), Cancun, Quintana Roo, Mexico, March 2011, pp. 1363–1368

[5] Han, S.H., Lee, J.H.: 'An overview of peak-to-average power ratio reduction techniques for multicarrier transmission', *IEEE Wirel. Commun. Mag.*, 2005, **12**, (2), pp. 56–65

[6] Singh, V., Sharma, R.: 'PAPR reduction techniques in LTE/LTE – a systems'. Proc. IEEE Int. Conf. on Advanced Communications Control and Computing Technologies (ICACCCT), Ramanathapuram, India, May 2014, pp. 688–692

[7] Vangala, S.K., Anuradha, S.: 'Analysis and comparison of clipping techniques for OFDM/OQAM peak-to-average power ratio reduction'. Proc. 2015 Int. Conf. on Applied and Theoretical Computing and Communication Technology (ICATCCT), Davangere, India, 2015, pp. 791–795

[8] Singh, S., Kumar, A.: 'A modified clipping algorithm for reduction of PAPR in OFDM systems'. Proc. 2015 IEEE Int. Conf. on Computational Intelligence and Computing Research (ICCIC), Madurai, India, 2015, pp. 1–4

[9] Udomsripaiboon, T.: 'Adjustable dynamic range for PAPR clipping technique in large-scale MIMO-OFDM systems'. Proc. 2018 Int. ECTI Northern Section Conf. on Electrical, Electronics, Computer and Telecommunications Engineering (ECTI-NCON), Chiang Rai, Thailand, 2018, pp. 25–28

[10] Ali, M., Rao, R.K., Parsa, V.: 'PAPR reduction in OFDM systems using clipping based on symbol statistics'. Proc. 2017 IEEE 30th Canadian Conf. on Electrical and Computer Engineering (CCECE), Windsor, ON, Canada, 2017, pp. 1–5

[11] Xin, Y., Fair, I.J.: 'Error-control selective mapping coding for PAPR reduction in OFDM systems'. Proc. IEEE 60th Vehicular Technology Conf., VTC2004-Fall, Los Angeles, CA, USA, 2004, vol. 1, pp. 583–587

[12] Shu, S., Qu, D., Li, L., *et al.*: 'Invertible subset QC-LDPC codes for PAPR reduction of OFDM signals', *IEEE Trans. Broadcast.*, 2015, **61**, (2), pp. 290–298

[13] Kang, K., Choi, K., Shin, S.K.: 'Reduced search for optimum code sets to reduce PAPR in MC-CDMA system'. Proc. The 5th Int. Symp. on Wireless Personal Multimedia Communications, Honolulu, HI, USA, 2002, vol. 1, pp. 135–139

[14] Jiang, T., Ni, C., Ye, C., *et al.*: 'A novel multi-block tone reservation scheme for PAPR reduction in OQAM-OFDM systems', *IEEE Trans. Broadcast.*, 2015, **61**, (4), pp. 717–722

[15] Chen, J.C., Li, C.P.: 'Tone reservation using near-optimal peak reduction tone set selection algorithm for PAPR reduction in OFDM systems', *IEEE Signal Process. Lett.*, 2010, **17**, (11), pp. 933–936

[16] Hou, J., Tellambura, C., Ge, J.: 'Clipping noise-based tone injection for PAPR reduction in OFDM systems'. Proc. 2013 IEEE Int. Conf. on Communications (ICC), Budapest, Hungary, 2013, pp. 5759–5763

[17] Yang, L., Soo, K.K., Siu, Y.M., *et al.*: 'A low complexity selected mapping scheme by use of time domain sequence superposition technique for PAPR reduction in OFDM system', *IEEE Trans. Broadcast.*, 2008, **54**, (4), pp. 821–824

[18] Naeiny, M.F., Marvasti, F.: 'Selected mapping algorithm for PAPR reduction of space-frequency coded OFDM systems without side information', *IEEE Trans. Veh. Technol.*, 2011, **60**, (3), pp. 1211–1216

[19] Badran, E.F., El-Helw, A.M.: 'A novel semi-blind selected mapping technique for PAPR reduction in OFDM', *IEEE Signal Process. Lett.*, 2011, **18**, (9), pp. 493–496

[20] Chen, J.C.: 'Application of quantum-inspired evolutionary algorithm to reduce PAPR of an OFDM signal using partial transmit sequences technique', *IEEE Trans. Broadcast.*, 2010, **56**, (1), pp. 110–113

[21] Varahram, P., Al-Azzo, W.F., Ali, B.M.: 'A low complexity partial transmit sequence scheme by use of dummy signals for PAPR reduction in OFDM systems', *IEEE Trans. Consum. Electron.*, 2010, **56**, (4), pp. 2416–2420

[22] Alavi, A., Tellambura, C., Fair, I.: 'PAPR reduction of OFDM signals using partial transmit sequence: an optimal approach using sphere decoding', *IEEE Commun. Lett.*, 2005, **9**, (11), pp. 982–984

[23] Wan, Y., Wang, Y.: 'Efficient PAPR reduction through random constellation mapping'. Proc. 2017 3rd IEEE Int. Conf. on Computer and Communications (ICCC), Chengdu, China, December 2017, pp. 2625–2628

[24] Shaheen, I.A., Zekry, A., Newagy, F., *et al.*: 'PAPR reduction of FBMC/OQAM systems based on combination of DST precoding and A-law nonlinear companding technique'. Proc. 2017 Int. Conf. on Promising Electronic Technologies (ICPET), Deir El-Balah, Palestine, October 2017, pp. 38–42

[25] Chen, H., Haimovich, A.M.: 'Iterative estimation and cancellation of clipping noise for OFDM signals', *IEEE Commun. Lett.*, 2003, **7**, (7), pp. 305–307

[26] Armstrong, J.: 'Peak-to-average power reduction for OFDM by repeated clipping and frequency domain filtering', *Electron. Lett.*, 2002, **38**, (8), pp. 246–247

[27] Nakamura, T.: 'Proposal for candidate radio interface technologies for IMT-advanced based on LTE release 10 and beyond (LTE-advanced)'. Paper presented on ITU-R WP5 D 3rd Work shop on IMT-Advanced, Dresden, Germany, October 2009

[28] Yuan, G.X., Zhang, X., Wang, W.B., *et al.*: 'Carrier aggregation for LTE-advanced mobile communication systems', *IEEE Commun. Mag.*, 2010, **48**, (2), pp. 88–93

[29] 3GPP Technical Report 36.808: 'Evolved universal terrestrial radio access (E-UTRA); carrier aggregation; base station (BS) radio transmission and reception (release 10)', v9.0.0, June 2012

[30] 3GPP Technical Report 36.815: 'LTE-advanced feasibility studies in RAN WG4 (release 9)', v9.1.0, June 2010

[31] Bassam, S.A., Chen, W.H., Helaoui, M., *et al.*: 'Transmitter architecture for CA: carrier aggregation in LTE-advanced systems', *IEEE Microw. Mag.*, 2013, **14**, (5), pp. 78–86

[32] Park, C.S., Sundstrom, L., Wallen, A., *et al.*: 'Carrier aggregation for LTE-advanced: design challenges of terminals', *IEEE Commun. Mag.*, 2013, **51**, (12), pp. 76–84

[33] Sundström, L., Anderson, M., Strandberg, R., *et al.*: 'A receiver for LTE Rel-11 and beyond supporting non-contiguous carrier aggregation'. Proc. IEEE Int. Solid-State Circuits Conf. Digest of Technical Papers (ISSCC), San Francisco, CA, USA, February 2013, pp. 336–337

[34] Ajami, A., Artail, H.A., Mansour, M.M.: 'A low-complexity PAPR reduction technique for LTE-advanced uplink with carrier aggregation'. Proc. 2015 IEEE Global Communications Conf. (GLOBECOM), San Diego, CA, USA, December 2015, pp. 1–6

[35] Zhong, X.M., Qi, J., Bao, J.: 'Using clipping and filtering algorithm to reduce PAPR of OFDM system'. Proc. Int. Conf. on Electronics, Communications and Control (ICECC), Ningbo, China, September 2011, pp. 1763–1766

[36] Srivastava, G.K., Tadkapalli, N.K.: 'Crest factor reduction for carrier aggregated OFDM systems'. Proc. IEEE Software, Telecommunication and Computer Networks (Softcom), Split, Croatia, September 2012, pp. 1–6

[37] Wang, Y.C., Luo, Z.Q.: 'Optimized iterative clipping and filtering for PAPR reduction of OFDM signals', *IEEE Trans. Commun.*, 2011, **59**, (1), pp. 33–37

[38] Zhu, X.D., Pan, W.S., Li, H., *et al.*: 'Simplified approach to optimized iterative clipping and filtering for PAPR reduction of OFDM signals', *IEEE Trans. Commun.*, 2013, **61**, (5), pp. 1891–1901

[39] Boyd, S., Vandenberghe, L.: '*Convex optimization*' (Cambridge University Press, New York, 2004)

[40] Grant, M., Boyd, S., Ye, Y.: 'CVX: Matlab Software for disciplined convex programming', 2006. Available at http://www.stanford.edu/~boyd/cvx/

[41] Guo, H., Burrus, C.S.: 'Wavelet transform based fast approximate Fourier transform'. Proc. IEEE Int. Conf. on Acoustics, Speech, and Signal Processing (ICASSP), April 1997, vol. 3, pp. 1973–1976